



Borislava Blagojević, University of Nis, borislava.blagojevic@gaf.ni.ac.rs  
Ajla Mulaomerović-Šeta, University of Sarajevo, ajla.mulaomerovic@gf.unsa.ba  
Vladislava Mihailović, University of Belgrade, vladislava.mihailovic@sfb.bg.ac.rs  
Andrea Petroselli, Tuscia University, petro@unitus.it

## REGIONALIZATION OF CATCHMENTS BASED ON SILHOUETTE WIDTHS FOR FLOOD RESPONSE ESTIMATION ACROSS SERBIA

### *Abstract*

Regional analysis is often used for flood quantile estimation in ungauged catchments. The regionalization procedure has two phases: the formation of homogeneous regions and flood quantile estimation. The presented research results consider the first phase of the regional analysis for 41 catchments in Serbia. The catchment similarity attributes are catchment area and catchment mean elevation. The number of formed regions and the number of stations within the regions are determined by maximising the mean silhouette width of the region. Regions were first obtained by cluster analysis and then adjusted to comprise catchments with a positive silhouette width. For the three formed regions, homogeneity was checked by the Gini index - GI.

*Keywords: regional analysis, Flood flow, Cluster analysis, silhouette width, Gini index*

## РЕГИОНАЛИЗАЦИЈА СЛИВОВА НА ОСНОВУ ШИРИНЕ СИЛУЕТЕ ЗА ОЦЈЕНУ ВЕЛИКИХ ВОДА НА ТЕРИТОРИЈИ СРБИЈЕ

### *Сажетак*

Регионална анализа се често користи за оцјену великих вода у неизученим сливовима. Поступак регионализације има две етапе: формирање хомогених региона и оцјену квантила великих вода. Приказани резултати истраживања баве се првом фазом регионалне анализе за 41 слив на територији Србије. Атрибути сличности сливова су површина и средња надморска висина слива. Број формираних региона и број станица у регионима одређени су према услову највеће могуће ширине силуете региона. Региони су добијени испрва кластер анализом, а затим су подешени тако да све станице у регионима имају позитивну ширину силуете. За три формирана региона, хомогеност је провјерена Џини индексом - GI.

*Кључне ријечи: регионална анализа, велике воде, кластер анализа, ширина силуете, GI*

## 1. INTRODUCTION

Accurate flood estimation is important in civil engineering and construction to design the structures such as bridges, assess and mitigate potential risks to infrastructure and public safety. By properly estimating flood levels, resilient structures and infrastructure are designed, reducing the likelihood of damage and the need for costly repairs. Additionally, precise flood estimation enables informed decision-making regarding land use planning and development, ensuring that projects are located in areas less susceptible to flooding, ultimately enhancing community resilience.

In gauged catchments, flood estimation relies on available data from hydrological and meteorological gauging stations, enabling more precise assessments due to direct measurements of streamflow and rainfall. However, in ungauged catchments, flood estimation is more challenging as there is limited or no data, necessitating the use of indirect methods such as rainfall-runoff models or regional flood frequency analysis to approximate flood flows and from them, corresponding flood levels.

Although regional flood frequency analysis is typically employed in situations where limited or no direct data on flood events are available for a specific location or catchment, it is also used in gauged catchments for control of flood quantile estimation results or statistical properties of flood data series (e.g. skewness [1]), and when long data is available but the data record length is inappropriate compared to desired return period of flood quantiles [2]. In these situations, additional data must be incorporated, and it involves expanding temporal, spatial, and causal information to refine flood quantile estimation.

The primary focus of this paper revolves around spatial data transfer, particularly employing regionalization methods to formation of homogeneous regions. Spatial information expansion encompasses two main techniques: spatial regionalization and statistical regionalization. Spatial regionalization involves constructing envelope curves, specific runoff diagrams, or maps depicting quantiles or statistical parameters. Envelope curves and specific runoff diagrams illustrate high flows relative to catchment area or river network segments, and assist in validating estimated flood flows. Statistical regionalization procedures involve establishing dependencies between the parameters or quantiles of flood flows and the morphological and/or meteorological characteristics of the catchment. Key stages in statistical regionalization include identifying homogeneous regions and transferring information, particularly for estimating flood flows. Various methods for regionalization exist in the literature, differing mainly in their approach to these two critical stages. Geographically adjacent regions are often presumed to exhibit similar hydrological processes and are thus treated as homogeneous areas for flood flow estimation, although this assumption may not always hold true [3]. To address this subjectivity, methods such as cluster analysis [4] or the Region of Influence (ROI) approach [5] are employed. In both cluster analyses and ROI, selecting attributes that reflect similarity among catchments is crucial. Typically, geomorphological characteristics are prioritized due to their accessibility [6], followed by hydro-meteorological properties [7] or the timing and distribution of peak flows [8], which offer more accurate and robust data.

Cluster analysis is commonly employed in flood regionalization due to its practicality [9], with Ward's algorithm (hierarchical approach) [10] or the k-means algorithm (partition approach) [11] being the most utilized methods. The hierarchical approach offers a dendrogram presentation of results, allowing for the determination of regions based on arbitrary distances or a specified number of cluster centers (CCs). Conversely, the partition approach requires predefining the number of CCs, often leading to dependency on initial assumptions and necessitating multiple runs of the algorithm. Despite the hierarchical approach's limitations regarding object migration between CCs, a hybrid cluster analysis has been proposed [4], combining both hierarchical and partition approaches to leverage their respective strengths.

In Bosnia and Herzegovina and Serbia, flood quantile estimation in ungauged catchments often relies on specific runoff diagrams or regressions linking flood quantiles with catchment area [12]. However, this approach has demonstrated notable tendencies for both underestimation and overestimation of flood quantiles, especially considering the assumption of homogeneous regions without validation [13]. Other techniques employed to enhance flood quantile estimation include extending gauged peak flow data using gauged water stage [14], assumed rating curves, and historical flood records [15]. Furthermore, comparative analyses involving statistical methods, empirical expressions, and geomorphological unit hydrographs such as the EBA4SUB model [16] have been considered. Regional analysis utilizing the cluster method was conducted for stations in Bosnia and Herzegovina, expanded to include stations from Serbia, highlighting the superiority of hierarchical (Ward's algorithm) over partition (k-means) clustering in flood quantile estimation [13].

In a recent research [17], an alternative hierarchical approach to region formation for flood quantile estimation was explored. The appropriateness of object assignment to a CC was evaluated using the silhouette width [18], while achieved mean silhouette width of a CC was used as a measure of optimal cluster number [19]. Regarding region formation, it is concluded in [17] that 1) the regions should be adjusted to comprise (hydrological gauging) stations with positive individual silhouette widths, and 2) the minimum number of stations in a region should be nine.

The aim of this paper is to investigate whether homogeneous flood estimation regions can be formed in Serbia with the minimum number of nine stations per region, based on silhouette widths. Additionally, it is examined if and how region adjustments influence selection of regional distribution function, i.e. information transfer function in each region.

The present work is partially based on the data and findings from the previous research [17]. The appropriateness of the silhouette-width-induced clustering is rated here using mean silhouette width as a measure of region compactness [18] and region homogeneity examination by the Gini Index (GI) [20], while preliminary detection of regional distribution function is done by L-moment plots.

## 2. METHODOLOGY

### 2.1. STUDY REGION AND DATA

The study region is situated in the southern part of the Danube River basin, in Serbia, and it is characterized by continental climate. The annual peak flow data were collected for 41 hydrological stations (HSs), with a catchment area up to 2054 km<sup>2</sup> (Figure 1).

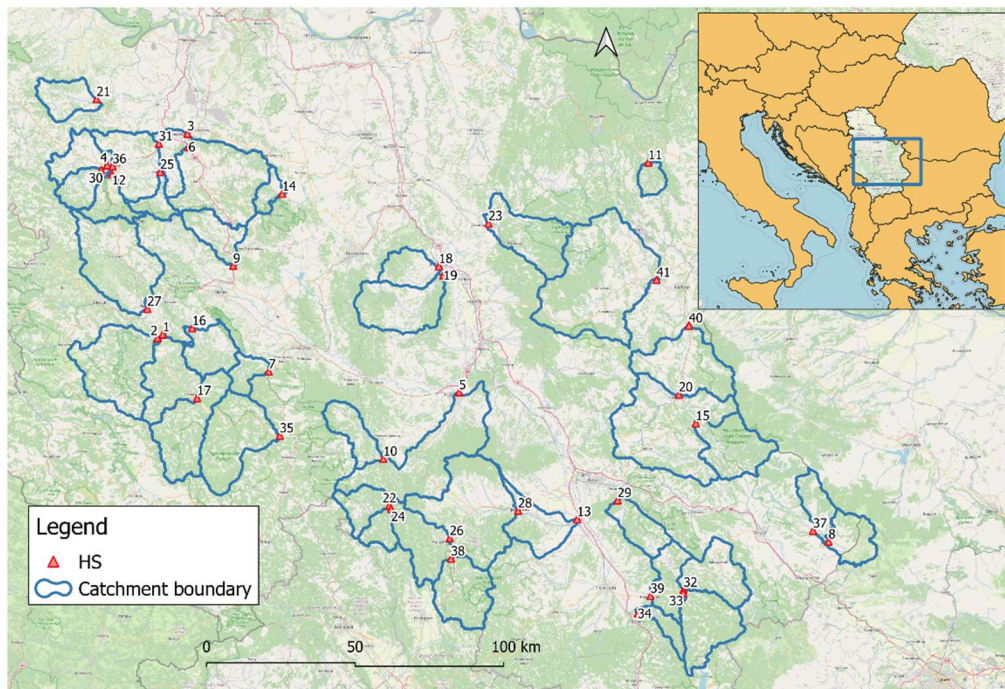


Figure 1. Study region, catchments and locations of hydrological gauge stations.

Statistical tests were conducted on peak flow datasets from 41 stations (Table 1) spanning the gauge period of 1948–2016, to assess their suitability for flood frequency analysis by statistical analysis of annual peak flows, focusing on stationarity, independence, and homogeneity in mean and variance [17]. In 12 stations, datasets were trimmed from the beginning of the gauge period until they met the criteria for statistical analysis, at the 5% significance level. The trimmed gauged peak flow data spanned from 1 to 22 years (Table 1). The datasets with gaps are left unaltered. On average, the datasets had a record length of 53 years.

The main catchment morphological attributes, such as catchment area ( $A$ ), average slope ( $I_{avg}$ ) and average elevation ( $H_{avg}$ ), have been determined from a 20 m resolution DEM [21].

Table 1. Annual peak flow data at stations: N-record length, Ntrimm-number of trimmed years in the data record, MAF- mean annual flood, LCv-L-coefficient of variation. Source [22].

Stat. no.	Station name	N	Ntrimm	MAF (m <sup>3</sup> /s)	LCv (-)	A (km <sup>2</sup> )	Iavg (%)	Havg (m asl)
1	Arilje	65		120.6	0.336	818	20.9	856
2	Arilje Rzav	49		100.1	0.258	583	25.4	870
3	Beli Brod	52	6	288.6	0.353	1833	19.83	373
4	Belo Polje	63		59.7	0.373	185	18.26	401
5	Bivolje	42	22	101.7	0.389	957	17.1	570
6	Bogovadja	59		99.3	0.328	697	14.1	314
7	Bogutovac	56		35.6	0.399	115	37.14	779
8	Brajicevci	54		40.0	0.352	227	21.7	1211
9	Brdjani	47		51.6	0.416	208	23.8	502
10	Brus	57		32.6	0.365	220	27.5	898
11	Crnajka	47	5	25.1	0.454	78	23.4	521
12	Degurici	55	3	44.1	0.356	159	29.8	673
13	Doljevac	58	5	135.5	0.350	2054	24.99	646
14	Donja Satornja	38	17	18.8	0.659	84	17.9	494
15	Donja Kamenica	61		44.2	0.408	360	36.62	812
16	Guca	54		71.2	0.341	235	22.2	576
17	Ivanjica	53		75.5	0.346	460	33.1	980
18	Jagodina	56		19.3	0.452	193	18.7	296
19	Jagodina Majur	53		73.3	0.502	427	21.35	390
20	Knjazevac	49	14	113.2	0.333	1260	26.2	659
21	Koceljeva	52	1	33.5	0.378	208	15.2	257
22	Magovo	42		30.1	0.430	180	33	1021
23	Man. Manasija	52		60.9	0.437	388	26.28	637
24	Mercez	45		19.6	0.425	112	44.7	1015
25	Pastric Mionica	58		50.4	0.550	108	28.27	530
26	Pepeljevac	46	20	130.4	0.336	987	26.1	800
27	Pozega	57		118.9	0.458	630	23.23	597
28	Prokuplje	42	20	151.4	0.367	1773	26.57	684
29	Radikine Bare	38	11	23.1	0.369	205	29	676
30	Sedlare	62		41.7	0.445	140	34.1	637
31	Slovac	59		187.9	0.297	995	20.1	443
32	Svodje Luznica	52		62.9	0.433	318	26.9	707
33	Svodje Vlasina	61		49.0	0.458	349	35.21	1066
34	Tupalovce	54		22.2	0.308	98	36.6	931
35	Usce Studenica	63		59.2	0.279	535	34.89	1130
36	Valjevo	59		85.8	0.378	340	12.96	510
37	Visocka.Rzana	42		69.9	0.314	403	32.23	1218
38	Visoka	55		71.2	0.422	370	28.9	740
39	Vlasotnice	57		147.3	0.400	972	28.7	865
40	Vratarnica	66		142.5	0.300	1765	25.72	614
41	Zajecar Gamzigrad	49	12	110.0	0.315	1167	19.83	528

## 2.2. METHODS

Regional analysis, regardless of employed methods, consists of two phases with 4 common steps:

- Phase 1:
  - Region (pooling region) formation,
  - Testing region homogeneity,
- Phase 2:
  - Information transfer function definition, and
  - Quantile estimation.

The focus of this research is in regional analysis phase 1, and in its results that influence the setup of the phase 2 for the Index-flood method, i.e. regional information transfer function.

The majority of calculations shown in the paper is performed in R package, ver 4.1.2.

### 2.2.1. REGION FORMATION

Within cluster analysis, catchments are assigned to regions via a hierarchical agglomerative process based on their morphological similarities. To prevent undue bias towards specific attributes, morphological characteristics should not display significant correlations [23]. Initially, each catchment forms its own cluster, with merging occurring progressively at each level of the clustering algorithm until a single region is formed. Ward's algorithm, chosen for its ability to create cohesive regions [4], is employed in this process.

The number of centers is selected according to the silhouette width, calculated as the ratio of the average distance of the object  $i$  from the others falling into the same center  $j$  and the maximum distance  $d$  from the objects of other centers [39]:

$$s_i^j = \frac{b_i^j - a_i^j}{\max(a_i^j, b_i^j)} \quad (1)$$

where  $s_i^j$  is the silhouette width of the object  $i$  from the cluster (center)  $j$ ,  $a_i^j$  is the average distance between  $i$ -th vector in cluster  $C_j$  and other vectors in the same cluster, and  $b_i^j$  is the minimum average distance between  $i$ -th vector in cluster  $C_j$  and other vectors in the remaining clusters  $C_k$  ( $k = 1, \dots, K, k \neq j$ ):

$$a_i^j = \frac{1}{m_j - 1} \sum_{\substack{k=1 \\ k \neq i}}^{m_j} d(X_i^j, X_k^j), \quad i = 1, \dots, m_j \quad (2)$$

$$b_i^j = \min_{\substack{n=1, \dots, K \\ n \neq j}} \left\{ \frac{1}{m_n} \sum_{\substack{k=1 \\ k \neq i}}^{m_n} d(X_i^j, X_k^j) \right\}, \quad i = 1, \dots, m_j \quad (3)$$

where  $d(X_i^j, X_k^j)$  is the distance between objects  $X_i$  and  $X_k$ ,  $m_j$  is the number of objects in cluster  $C_j$ ,  $m_n$  is the number of objects in remaining clusters  $C_k$ , and  $K$  is the number of cluster centers.

The silhouette width, ranging from -1 to 1, indicates the compactness of a cluster, with values closer to 1 indicating greater cohesion and suitability for assignment to a center. The determination of the optimal number of centers is achieved by maximizing the mean silhouette width (MSW) of all objects in the cluster. However, an inherent challenge of this method arises from silhouette widths approaching zero or turning negative. In the latter case, negative values signify misplacement within a center, prompting adjustments to reassign objects to achieve positive silhouette widths. This iterative process involves checking and potentially relocating objects until all silhouette widths are positive, ensuring the validity of cluster assignments.

### 2.2.2. REGION HOMOGENEITY TESTING

Region homogeneity testing refers to assessing whether the characteristics or attributes of a particular catchment are statistically similar or different from those in surrounding ones in the cluster of catchments. In statistical regionalization, this testing implies determining a certain measure that describes deviations in distribution functions or statistical parameters. The most frequently used region homogeneity tests in hydrology are the parametric Hosking–Wallis (HW) test, and the Anderson–Darling (AD) bootstrap test, explained in detail in [17]. In this paper, Gini index (GI) is used as a measure of region homogeneity. The GI, originally designed as a measure in the field of economics (econometrics), is adopted by Raquena et al. [20] to measure region heterogeneity in regional hydrological frequency analysis, in the following form:

$$GI = \frac{\sum_{i=1}^N (2i-N-1)t_{i:n}}{N(N-1)\bar{t}} \quad (4)$$

where  $t_{i:n}$  are the sample order statistics of  $L$ -coefficient of variation (usually labeled as  $t$ ),  $\bar{t}$  is their mean,  $N$  is number of stations in the region with data length  $n$ . This measure corresponds to the approach based on moments [24] where the coefficient of variation is used for defining homogeneous region when of 0 value and showing extremely heterogenous region when  $\geq 0.4$ . However, the GI does not provide a critical value, but its specific values between 0 and 1 are interpreted depending on the context and the distribution being measured.

The data required for GI estimation ( $L$ -moments of each dataset) are tabulated in [17] Appendix A, while  $t$ , i.e.  $LCv$  is given in Table 1.

Regional  $L$ -moments  $t^R$ ,  $t_3^R$  and  $t_4^R$  i.e. regional  $L$ -variation coefficient,  $L$ -skewness, and  $L$ -kurtosis respectively, are derived as average values, weighted by dataset size as:

$$t^R = LCv = \frac{\sum_{i=1}^{m_j} n_i t^{(i)}}{\sum_{i=1}^{m_j} n_i} \quad (5)$$

$$t_3^R = LCs = \frac{\sum_{i=1}^{m_j} n_i t_3^{(i)}}{\sum_{i=1}^{m_j} n_i} \quad (6)$$

$$t_4^R = Lck = \frac{\sum_{i=1}^{m_j} n_i t_4^{(i)}}{\sum_{i=1}^{m_j} n_i} \quad (7)$$

where  $i$  is station in region  $R$  of size  $m_j$ ,  $n_i$  is  $i$ -th station's record length.

### 2.2.3. PRELIMINARY SELECTION OF REGIONAL DISTRIBUTION

To identify the appropriate distribution (or several candidates), plots of dimensionless  $L$ -moments proposed by Hosking [25] are used here. They show the relationship between  $LCv$  and  $LCs$  for two-parameter, i.e.  $Lck$  and  $LCs$  for three-parameter distributions (Figure 2). The closeness of the point representing  $L$ -moments of the studied dataset signifies an appropriate 2-parameter distribution when it is close to the marker in Figure 2, and/or 3-parameter distribution when close to the line. The red dot representing regional  $L$ -moments values in Figure 2 shows that the best distribution for a particular dataset would be 3-parameter generalized logistic distribution (GLO).

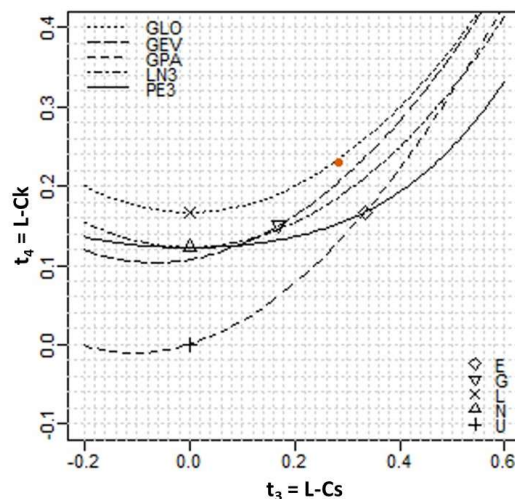


Figure 2.  $L$ -moments plot.

## 3. RESULTS

### 3.1. REGION FORMATION

In the formation of regions, catchment similarity attributes, clustering algorithm and number of centres are defined. The catchment morphological attributes that do not display significant

correlations are found to be catchment area ( $A$ ) and average catchment elevation ( $H_{avg}$ ). Therefore, input data for cluster analysis is Euclidean distance matrix (Figure 3), derived based on normalized values of  $A$  and  $H_{avg}$ .

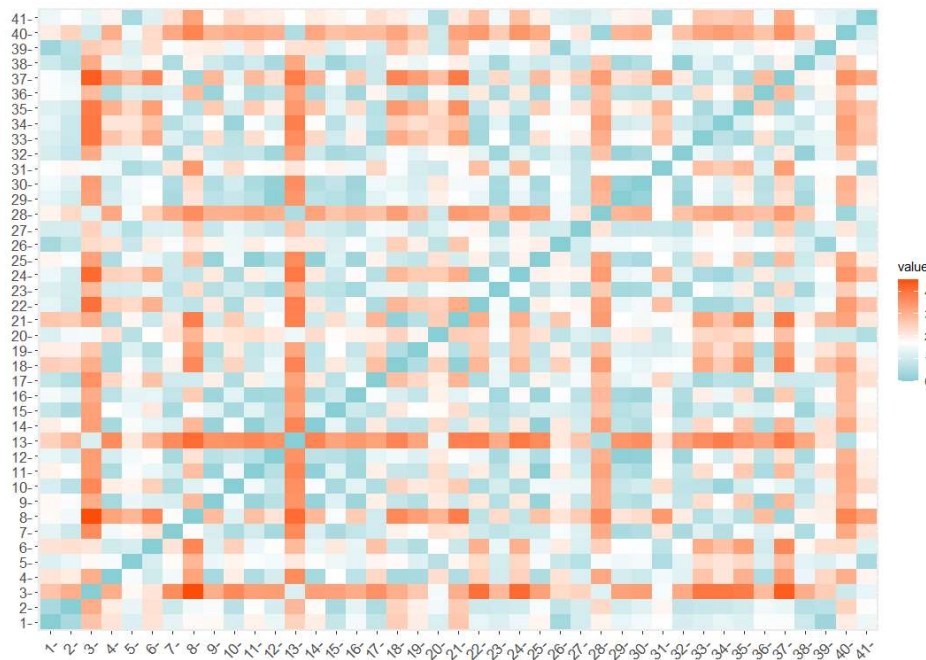


Figure 3. Catchment morphologic attributes distance matrix for catchment area ( $A$ ) and average basin elevation ( $H_{avg}$ )

The result of the cluster analysis performed by Ward's algorithm is presented in the dendrogram form (Figure 4).

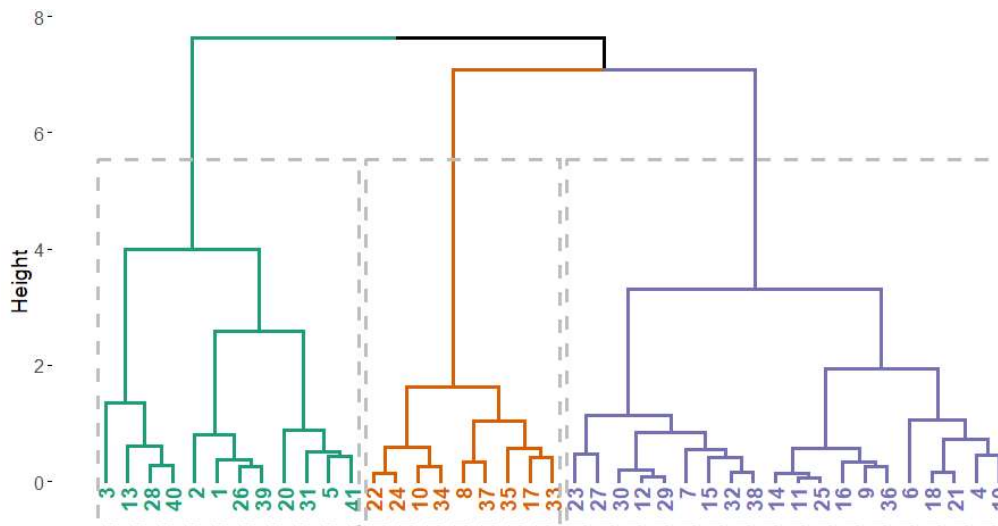


Figure 4. Cluster dendrogram based on Ward's clustering algorithm for 41 stations according to catchment similarity attributes, shown by their labels as in Table 1.

Based on the results of hierarchical grouping (dendrogram), regions are formed by choosing the number of centers. According to 23 measures available in *NbClust* function in R [26], 9 measures (the largest share of all measures) proposed 3 as the best number of clusters, and according to the 'majority rule', as defined in R package, that is the best number of CCs. Considering silhouette width measure alone, four, followed by three, is the best number of CCs (Table 2).

Table 2. Mean silhouette width (MSW) change with number of cluster centers (CC).

CCs	2	3	4	5	6	7	8	9	10
MSW	0.3663	<b>0.4484</b>	<b>0.4491</b>	0.4075	0.4332	0.4289	0.4097	0.4305	0.4254

When four CCs are considered according to MSW, there are 4, 8, 9 and 20 stations in the CCs respectively. Because the first two CCs hold less than 9 stations in the CC, which is set as a target in this paper, and MSWs for three CCs and four CCs are almost the same (0.4484 and 0.4491), the final number of CCs is set to three. The size of adopted three regions is 9, 12, and 19 stations (Figure 5).

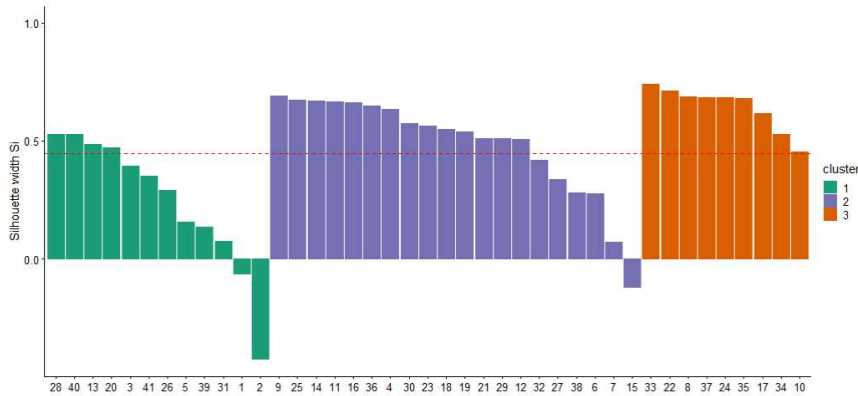


Figure 5. Cluster silhouette width plot for three adopted CCs

### 3.2. ADJUSTMENT OF REGIONS

The optimal number of CCs is achieved by maximizing the MSW of all objects in the cluster. Such clustering is labelled ORG hereinafter. Negative silhouette width of individual object (station) in the CC signify misplacement within a center, requiring adjustments to reassign object to another CC to achieve positive silhouette width. In Figure 6, it may be seen that three stations exhibit negative silhouette widths. The adjustment of CCs (regions) starts with the station of the largest negative silhouette width, station no. 2. Relocating one station to another CC changes the silhouette widths of all stations. It took 5 iterations to reach positive silhouette widths for all stations, forming adjusted regions (labelled ADJ). Five stations are moved to adj\_CC3 (four from CC1 and one from CC2). Silhouette widths for original and adjusted regions are shown in Figure 6.

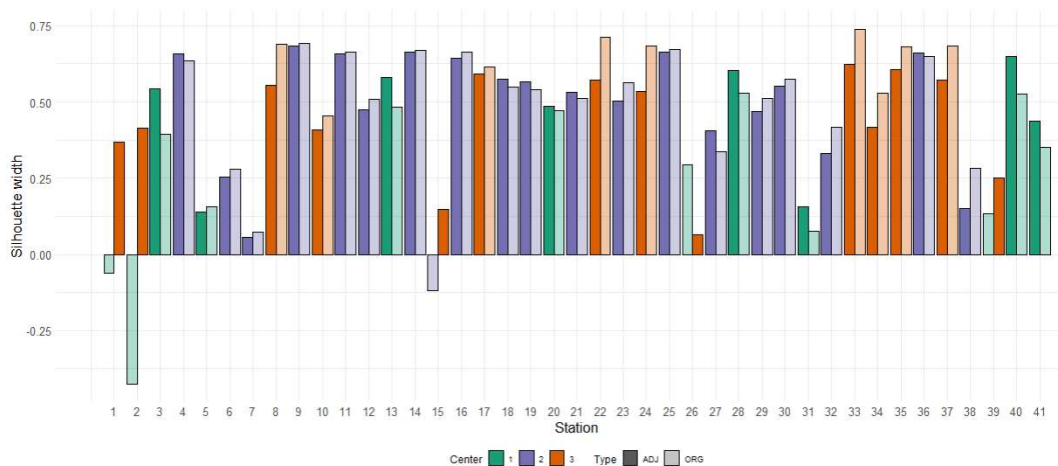


Figure 6. Single silhouette width per station in the original (transparent bar colour) and adjusted clusters (solid bar colour).

Table 3 shows that MSW is improved in adjusted CCs 1 and 2 compared to original, while the adjusted CC3 has turned from the highest MSW to the lowest one. On average, MSW of all stations is improved by the adjustments, compared to the original placement of stations in the CCs (Table 3, column ‘Overall’).



The change in morphological attributes across CCs in ADJ clustering compared to ORG is shown in Figure 7. Both methods (ORG and ADJ) pooled stations with larger basin area into CC1 (Figure 7 – left). A significant distinction between CC2 and CC3 (regions with smaller and medium catchment area) is in the average catchment altitudes, shown by a visible departure of CC3 from other clusters in both ORG and ADJ clustering (Figure 7 – right).

Table 3. Mean silhouette width achieved in each CC and in all stations. Number of stations (region size) is given in the brackets below the MSW value.

Method	CC1	CC2	CC3	Overall
ORG	0.244 (12)	0.484 (19)	0.643 (9)	0.448
ADJ	0.450 (8)	0.500 (18)	0.438 (14)	0.469



Figure 7. The boxplots of morphological attributes in the original and adjusted clusters mapped by the CC: CC1 – green, CC2 – purple, CC3 - orange.

The principal component (PC) plots in Figure 8, visualize the change of CC gravity centers location (in the first two PC dimensions) caused by ADJ clustering, as well as the change in shapes of the three CCs. It may be seen that CC3 significantly grew on the account of CC1 in ADJ clustering.

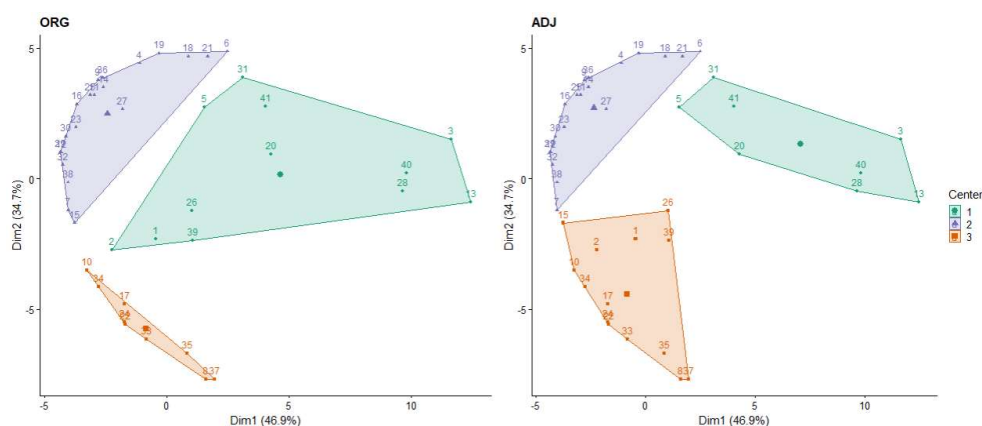


Figure 8. Principal component plots for the original (left) and adjusted (right) CCs.

### 3.3. REGION HOMOGENEITY

The GI values are shown in Table 4 for regions formed by cluster analysis by both ORG and ADJ approach. The comparison of the individual GI values among regions reflects varying degrees of inequality within a CC. In general, equality in CCs, hence homogeneity, is improved by ADJ clustering, although the starting GI values in ORG CCs were already low, considering the GI range between 0 and 1. The most homogeneous region measured by the GI comprises stations in CC1, then CC2, and finally CC3 in ORG clustering, while in ADJ clusters, CC1 remained more homogeneous compared to CC2 and CC3 that are equalized by the adjustment.

Table 4. Gini index achieved in each CC upon ORG and ADJ clustering

Method	CC1	CC2	CC3
ORG	0.070	0.100	0.101
ADJ	0.058	0.101	0.098

The regional  $L$ -moments  $t^R$ ,  $t_3^R$  and  $t_4^R$  values estimated from flood flow (annual maxima) datasets according to equations (5), (6), and (7) in CCs are tabulated in Table 5. In CC1 and CC3 in both ORG and ADJ clusters, regional  $L$ -Cv is similar, while it is somewhat higher in CC2. The degree of variation within the clusters judged by  $L$ -Cv (Table 5) is different compared to GI in Table 4, where the least variation is found in CC1, then CC3 and the highest in CC2, regardless of the clustering method.

Table 5. Regional  $L$ -moments in CCs for ORG and ADJ clustering

Method	$L$ -moment	CC1	CC2	CC3
ORG	$L-Cv = t^R$	0.3348	0.4245	0.3625
	$L-Cs = t_3^R$	0.2850	0.3971	0.4064
	$L-Ck = t_4^R$	0.2291	0.2723	0.3001
ADJ	$L-Cv = t^R$	0.3345	0.4256	0.3583
	$L-Cs = t_3^R$	0.2758	0.3956	0.3775
	$L-Ck = t_4^R$	0.2265	0.2677	0.2865

### 3.4. REGIONAL THEORETICAL DISTRIBUTION FUNCTION

The  $L$ -moments plot, representing an aid in the final selection of regional distribution function, is provided in Figure 9. Compared to Figure 2, a part that fits the estimated  $L$ -moments values is zoomed, to provide better insight into transition of ADJ CCs relative to ORG CCs. The data used to plot points describing location of CCs in this respect are given in Table 5.

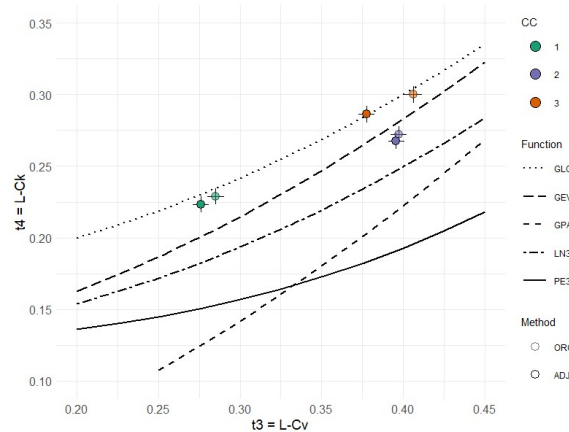


Figure 9.  $L$ -moments plot for the CCs of ORG (transparent marker) and ADJ (solid marker) clustering.

According to  $L$ -moments plot in Figure 9, the selection of regional distribution function is brought down to two: general logistic (GLO) and general extreme value (GEV) theoretical distribution. GLO is the best fit for CC1 and CC3, while GEV is the most suitable for CC2, and this holds for both ORG and ADJ clustering methods.

## 4. DISCUSSION

Following the aim of this research that is to investigate whether homogeneous flood estimation regions can be formed in Serbia with the minimum number of nine stations per region based on silhouette widths, it can be said that the main challenge in this research compared to others is the

available number of catchments, which is 41. According to the silhouette width classes of compactness [18], the ones achieved here for the three regions in the original clustering belong to weak ( $\geq 0.26$ ) to strong clustering class ( $\geq 0.51$ ), which changed to weak clustering after the adjustment of regions (0.450, 0.500 and 0.438). Nevertheless, the achieved results seem better than for 3 regions obtained for regionalization of 245 catchments in Indiana, USA, where the maximum silhouette value of 0.406 is obtained employing Ward's algorithm [27], and also for 555 stations in Slovakia and Austria, divided into 3 regions by the k-means algorithm, where the maximum silhouette width below 0.5 was reached [28]. On the other hand, regionalization of 27 mountainous catchments in Utah, USA, resulted in larger silhouette width (maximum value about 0.65), applying Wards' over k-means clustering, that was reached for 2 centres [27] exhibiting a strong clustering structure. However, in one region there were only 2 catchments, which is not enough for further regionalization (phase 2) bearing in mind minimum number of stations in the region set in this research.

Silhouette width approach based on average within-cluster distance (equation (1)) combines two clustering criteria, compactness and separation, which, according to Lengyel and Botta-Dukát [29], implies that spherical cluster shapes are preferred over others. This can also be seen in the PC plot shown in Figure 8 of our research by the shape before (Figure 8a) and after the adjustment (Figure 8b), where an overall mean silhouette width is improved in ADJ compared to ORG clustering, reflecting in more balanced shapes of the regions showing three cluster centres. For the future research, a new method using generalized mean with flexible formula [29] is going to be tested, that permits the adjustment of sensitivity within the formula through one parameter, to delineate the significance attributed to connectedness and compactness. In this way, better scores can be obtained for clusters that are not perfectly spherical [29]. Due to specific issues in flood response regionalization, the generalized mean functionality can be used to tailor classifications according to the significance of connectedness relative to compactness.

Silhouette width and, as a consequence, the optimal number of cluster centres, depend on the clustering algorithm [27] [30], as well as selected similarity attributes. Using the same number of catchments for flood related regionalization, but without silhouette width as a criterion, 41 catchments in Iran were regionalized by 8 methods using 8 similarity attributes (7 morphological and 1 meteorological) [31]. Evaluation of methods and similarity attributes is performed in terms of homogeneity, accuracy of flood quantiles and region size. Ten best cases according to region homogeneity include catchment area and main stream slope, while ten best cases according to accuracy are obtained for the main stream slope. In the final regionalization ranking, 7 out of 10 include main stream slope, and 3 of 10 include catchment area. It is to be expected that the main stream slope is a function of the catchment slope, that is found significantly correlated with the mean altitude in our research. Implicitly, our selection of catchment area and average basin elevation as catchment similarity attributes is confirmed in [31].

The adjustments of regions performed in the paper according to silhouette widths, have led to regions with more compact, evenly distributed geomorphological attributes: catchment area and mean elevation (Figure 7). Such a distribution of geomorphological attributes shown by box plots across regions is precondition for reliable linear regression equations between geomorphological attributes and flood characteristics, intended for the second phase of regional analysis, i.e. index-flood method. When it comes to region homogeneity, the lowest GI values are found in CC1 for both ORG and ADJ clustering methods, i.e. for regions consisting of large area catchments, while for CC2 and CC3, consisting of smaller area catchments in the study sample, GI is larger, pointing out to less homogeneous regions. The effect of adjustment of CC3 (adding 4 stations) contributed to slight reduction of GI. Merz and Blöschl [32] also found that by increasing catchment area the variation of  $C_v$  decreases (and consequently  $LC_v$ ), resulting in low GI. A large discrepancy in  $C_v$  is found in small catchments susceptible to flash floods, posing a challenge for establishing regression with the catchment area [32]. In general, it is considered that the regionalization of small catchments is a particularly difficult task partly due to the non-linear relationship between precipitation and runoff [33]. According to Raquena et al. results [20], it can be concluded that CC2 and CC3 are possibly homogeneous regions. The values of 0.1 of GI resemble to the range of 1 to 2 of  $HI$  in the Hosking and Wallis (HW) procedure, that gives inconclusive results regarding region homogeneity. Therefore, the final decision about adequacy of proposed regions is to be made according to flood quantile estimates, as in [17] and [31].

Additionally, it was found that adjustment of regions does not influence selection of distribution function according to L-moments plot i.e. information transfer function in each region, intended for index-flood method. It is worth noting that GLO (CC1, CC3) is recommended for regional

distribution function in the UK for the index-flood procedure [34], while GEV (CC2) has shown as the best selection in majority of European countries [35] for at-site flood frequency analysis.

## 5. CONCLUSIONS

The flood information transfer from gauged to ungauged catchments based on geomorphological similarity implies the formation of homogeneous regions, for which cluster methods are often used. In this research, the regionalization of catchments using the hierarchical procedure by the Ward's algorithm and its adjustment is performed through silhouette width approach, with the evaluation of the region homogeneity using the Gini index. The study region comprised 41 catchments in Serbia, with the catchment area between 78 and 2054 km<sup>2</sup>, and the average catchment elevation ranging from 257 to 1218 m a.s.l., as two catchment similarity attributes. In the first run of the clustering algorithm, three flood response estimation regions were formed with 9, 12 and 19 stations respectively, while after adjustment of regions according to silhouette widths, the regions comprised of 8, 18, and 14 stations.

The conclusions are as follows:

1. The intended number of stations in the flood response regions is achieved by original clustering, but with the adjustment, in one of the regions, there are 8 instead of 9 stations. This may not pose a problem in the index-flood procedure for flood quantile estimates, when establishing relationship between mean annual flood and catchment area. However, this has to be confirmed in further investigation.
2. The adjustment of regions according to silhouette widths had positive effects on the distribution of catchment morphological attributes within regions, compactness of regions, and generally on region homogeneity measure, the Gini Index. The adjustment had no influence on the theoretical probability distributions – general logistic and general extreme values, as candidates for regional transfer function compared to the original regions. These two functions are commonly used in at-site flood frequency analyses.
3. A significant improvement of the Gini index was noted in clusters that mainly consist of stations of larger catchment areas, while in regions with smaller catchment areas the value was slightly improved by the adjustments of regions.
4. The evaluation of flood response region homogeneity through Gini Index is simple and complements further regional analysis requirements through L-moments. Still, the space for inconclusiveness exists as in other known homogeneity tests applied in hydrology.

Further research will include performance-based evaluation i.e. the accuracy achieved in flood quantile estimation in the second regionalization phase, while including one meteorological catchment similarity attribute, and applying a new method using generalized mean instead of original method with mean silhouette width.

## ACKNOWLEDGEMENT

This research was partially funded by the Ministry of Science, Technological Development and Innovation of the Republic of Serbia, grant numbers 451-03-65/2024-03/ 200095, and 451-03-65/2024-03/ 200169.

## LITERATURE

- [1] England, J.F., Jr.; Cohn, T.A.; Faber, B.A.; Stedinger, J.R.; Thomas, W.O., Jr.; Veilleux, A.G.; Kiang, J.E.; Mason, R.R. Bulletin 17C Guidelines for Determining Flood Flow Frequency, Chapter 5 of Section B, Surface Water, Book 4, Hydrologic Analysis and Interpretation; U.S. Geological Survey: Reston, VA, USA, 2019
- [2] G. Blöschl and Deutsche Vereinigung für Wasserwirtschaft, Abwasser und Abfall, Eds., Ermittlung von Hochwasserwahrscheinlichkeiten (Determination of flood probabilities), [Stand:] August 2012. in DWA-Regelwerk Merkblatt, no. DWA-M 552. Hennef: DWA, Dt. Vereinigung für Wasserwirtschaft, Abwasser u. Abfall, 2012.
- [3] B. Blagojević and J. Plavšić, 'A normalized regression based regional model for generating flows at ungauged basins', *Water Sci. Technol. J. Int. Assoc. Water Pollut. Res.*, vol. 68, no. 1, pp. 99–108, 2013, doi: 10.2166/wst.2013.216.
- [4] R. Rao and Srinivasan, Regionalization of Watersheds An Approach Based on Cluster Analysis, vol. 58. in *Water Science and Technology Library*, vol. 58. Dordrecht: Springer Netherlands, 2008. doi: 10.1007/978-1-4020-6852-2.

- [5] Z. Zrinji and D. H. Burn, 'Flood frequency analysis for ungauged sites using a region of influence approach', *J. Hydrol.*, vol. 153, no. 1, pp. 1–21, Jan. 1994, doi: 10.1016/0022-1694(94)90184-8.
- [6] B. Blagojevic, 'Razvoj modela za prostornu interpolaciju hidroloških vremenskih serija na neizučenim profilima. (Development of a model for spatial interpolation of hydrologic time series in ungauged catchments) Ph. D. thesis.' University of Niš, Faculty of Civil Engineering and Architecture: Niš, Serbia, 2011.
- [7] T. D. Mengistu, T. A. Feyissa, I.-M. Chung, S. W. Chang, M. B. Yesuf, and E. Alemayehu, 'Regional Flood Frequency Analysis for Sustainable Water Resources Management of Genale–Dawa River Basin, Ethiopia', *Water*, vol. 14, no. 4, Art. no. 4, Jan. 2022, doi: 10.3390/w14040637.
- [8] T. B. M. J. Ouarda, J. M. Cunderlik, A. St-Hilaire, M. Barbet, P. Bruneau, and B. Bobée, 'Data-based comparison of seasonality-based regional flood frequency methods', *J. Hydrol.*, vol. 330, no. 1, pp. 329–339, Oct. 2006, doi: 10.1016/j.jhydrol.2006.03.023.
- [9] J. R. M. Hosking and J. R. Wallis, *Regional Frequency Analysis: An Approach Based on L-Moments*. Cambridge: Cambridge University Press, 1997. doi: 10.1017/CBO9780511529443.
- [10] K. Komi, B. A. Amisigo, B. Diekkrüger, and F. C. C. Hountondji, 'Regional Flood Frequency Analysis in the Volta River Basin, West Africa', *Hydrology*, vol. 3, no. 1, Art. no. 1, Mar. 2016, doi: 10.3390/hydrology3010005.
- [11] J. Parajka et al., 'Seasonal characteristics of flood regimes across the Alpine–Carpathian range', *J. Hydrol.*, vol. 394, no. 1, pp. 78–89, Nov. 2010, doi: 10.1016/j.jhydrol.2010.05.015.
- [12] H. Hrelja, 'Definiranje nekih elemenata hidrološkog režima metodom regionalizacije', *Vodoprivreda*, vol. 37, pp. 21–34, 2005.
- [13] A. Mulaomerović-Šeta, B. Blagojević, Š. Imširović, and B. Nedić, 'Assessment of Regional Analyses Methods for Spatial Interpolation of Flood Quantiles in the Basins of Bosnia and Herzegovina and Serbia', in *Advanced Technologies, Systems, and Applications VI*, N. Ademović, E. Mujčić, Z. Akšamija, J. Kevrić, S. Avdaković, and I. Volić, Eds., in *Lecture Notes in Networks and Systems*. Cham: Springer International Publishing, 2022, pp. 430–456. doi: 10.1007/978-3-030-90055-7\_35.
- [14] A. Mulaomerović-Šeta, B. Blagojević, V. Mihailović, and Ž. Lozančić, 'Flood Frequency Assessment in Data Poor Environment Case Study Maglaj-Poljice on the River Bosna'.
- [15] Radić, Z. Istorijaska poplava na Gornjoj Drini 1896 godine , *Zbornik radova sa 16. naučnog savetovanja Srpskog društva za hidraulička istraživanja (SDHI) i Srpskog društva za hidrologiju (SDH)*, Donji Milanovac, 22-23. oktobra 2012. Editors: Marko Ivetić, Radomir Kapor, Jasna Plavšić. pp. 605- 618. Univerzitet u Beogradu - Građevinski fakultet: Beograd, Srbija, 2012. ISBN 8675181590, 9788675181590.
- [16] A. Petroselli, A. Mulaomerović-Šeta, and Ž. Lozančić, 'Comparison of methodologies for design peak discharge estimation in selected catchments of Bosnia and Herzegovina', vol. 71, no. 9, Accessed: Feb. 23, 2023. [Online]. Available: <http://www.casopis-gradjevinar.hr/archive/article/2611>
- [17] A. Mulaomerović-Šeta, B. Blagojević, V. Mihailović, and A. Petroselli, 'A Silhouette-Width-Induced Hierarchical Clustering for Defining Flood Estimation Regions', *Hydrology*, vol. 10, no. 6, Art. no. 6, Jun. 2023, doi: 10.3390/hydrology10060126.
- [18] P. J. Rousseeuw, 'Silhouettes: A graphical aid to the interpretation and validation of cluster analysis', *J. Comput. Appl. Math.*, vol. 20, pp. 53–65, Nov. 1987, doi: 10.1016/0377-0427(87)90125-7.
- [19] M. Shutaywi and N. N. Kachouie, 'Silhouette Analysis for Performance Evaluation in Machine Learning with Applications to Clustering', *Entropy*, vol. 23, no. 6, Art. no. 6, Jun. 2021, doi: 10.3390/e23060759.
- [20] A. I. Requena, F. Chebana, and T. B. M. J. Ouarda, 'Heterogeneity measures in hydrological frequency analysis: review and new developments', *Hydrol. Earth Syst. Sci.*, vol. 21, no. 3, pp. 1651–1668, Mar. 2017, doi: 10.5194/hess-21-1651-2017.
- [21] Š. Imširović, 'Regionalna analiza karakteristika velikih voda na teritoriji Srbije i Bosne i Hercegovine u periodu 1961-1990 - Master thesis'. Univerzitet u Sarajevu- Građevinski fakultet.
- [22] A. Mulaomerović-Šeta, 'Primjena regionalnih analiza u cilju poboljšanja karakterisitka velikih voda - Ph. D. thesis'. University of Sarajevo- Faculty of Civil Engineering: Sarajevo, Bosnia and Herzegovina, 2022.

- [23] 'Cluster Analysis Gets Complicated', TRC Market Research. Accessed: Feb. 26, 2023. [Online]. Available: <https://trcmarketresearch.com/whitepaper/cluster-analysis-gets-complicated/>
- [24] J. R. Stedinger and L.-H. Lu, 'Appraisal of regional and index flood quantile estimators', *Stoch. Hydrol. Hydraul.*, vol. 9, no. 1, pp. 49–75, Mar. 1995, doi: 10.1007/BF01581758.
- [25] J. R. M. Hosking, 'L-Moments: Analysis and Estimation of Distributions Using Linear Combinations of Order Statistics', *J. R. Stat. Soc. Ser. B Methodol.*, vol. 52, no. 1, pp. 105–124, Sep. 1990, doi: 10.1111/j.2517-6161.1990.tb01775.x.
- [26] M. Charrad, N. Ghazzali, V. Boiteau, and A. Niknafs, 'NbClust: An R Package for Determining the Relevant Number of Clusters in a Data Set', *J. Stat. Softw.*, vol. 61, pp. 1–36, Nov. 2014, doi: 10.18637/jss.v061.i06.
- [27] E. Sharghi, V. Nourani, S. Soleimani, and F. Sadikoglu, 'Application of different clustering approaches to hydroclimatological catchment regionalization in mountainous regions, a case study in Utah State', *J. Mt. Sci.*, vol. 15, no. 3, pp. 461–484, Mar. 2018, doi: 10.1007/s11629-017-4454-4.
- [28] R. Markova, 'Identification of catchment with similar flood characteristics in the Alpine-Charpatian basins', presented at the 17th International Multidisciplinary Scientific GeoConference SGEM2017, Nov. 2017. doi: 10.5593/sgem2017H/33/S12.050.
- [29] A. Lengyel and Z. Botta-Dukát, 'Silhouette width using generalized mean—A flexible method for assessing clustering efficiency', *Ecol. Evol.*, vol. 9, no. 23, pp. 13231–13243, 2019, doi: 10.1002/ece3.5774.
- [30] A. Ramachandra Rao and V. V. Srinivas, 'Regionalization of watersheds by hybrid-cluster analysis', *J. Hydrol.*, vol. 318, no. 1, pp. 37–56, Mar. 2006, doi: 10.1016/j.jhydrol.2005.06.003.
- [31] A. Ahani, S. S. Mousavi Nadoushani, and A. Moridi, 'A ranking method for regionalization of watersheds', *J. Hydrol.*, vol. 609, p. 127740, Jun. 2022, doi: 10.1016/j.jhydrol.2022.127740.
- [32] R. Merz and G. Blöschl, 'A process typology of regional floods', *Water Resour. Res.*, vol. 39, no. 12, p. 2002WR001952, Dec. 2003, doi: 10.1029/2002WR001952.
- [33] J. Plavšić, *Inžinjerska hidrologija*, Građevinski fakultet Univerziteta u Beogradu.
- [34] Institute of Hydrology (1999) *Flood Estimation Handbook* (five volumes). Centre for Ecology & Hydrology
- [35] A. Castellarin et al., 'Review of applied-statistical methods for flood-frequency analysis in Europe', *Rev. Appl.-Stat. Methods Flood-Freq. Anal. Eur.*, Jan. 2012.